

PIWI-Interacting RNAs in Gliomagenesis: Evidence from Post-GWAS and Functional Analyses

Daniel I. Jacobs¹, Qin Qin¹, Michael C. Lerro¹, Alan Fu¹, Robert Dubrow², Elizabeth B. Claus³, Andrew T. DeWan², Guilin Wang⁴, Haifan Lin⁵, and Yong Zhu¹

Abstract

Background: PIWI-interacting RNAs (piRNAs), the largest class of noncoding RNAs in mammals, cooperate with PIWI proteins to safeguard the genome from insertional mutations during germline development. Although a growing number of studies have linked the PIWI-piRNA pathway to carcinogenesis, the role of piRNAs in glioma has not been explored.

Methods: Utilizing directly measured and imputed genotypes from the GliomaScan genome-wide association study (1,840 cases and 2,401 controls), genetic variants in 1,428 piRNAs were analyzed for association with glioma risk. *In vitro* assays were performed to interrogate the functional impact of a top identified piRNA and its variant allele.

Results: Variants in five piRNAs were considered to be associations of interest and four of these showed narrow clusters of enhanced association signals surrounding the index variant. Functional analyses of one of these piRNAs, piR-598, revealed that transfection of the wild-type piRNA impacted expression of

genes involved in cell death/survival and reduced glioma cell viability and colony formation. However, upon delivery of piR-598 containing the variant allele at rs147061479 [OR, 1.80; 95% confidence interval (CI), 1.33–2.46; $P = 1.69 \times 10^{-4}$], cell proliferation was sharply increased.

Conclusions: The genetic association analysis identifies several piRNAs associated with glioma risk, and follow-up functional analyses suggest that variant rs147061479 in piR-598 increases glioma risk by abolishing the tumor-suppressive function of piR-598, instead conferring growth-promoting properties.

Impact: This transdisciplinary study demonstrates a role of piRNAs in gliomagenesis by evidence from both post-GWAS and *in vitro* functional analyses and supports expanded investigation into the link between the PIWI-piRNA pathway and cancer. *Cancer Epidemiol Biomarkers Prev*; 25(7); 1073–80. ©2016 AACR.

Introduction

An emerging area of cancer research concerns the putative involvement of PIWI-interacting RNAs (piRNAs), which are small (mostly 26–32 nt) noncoding RNAs with millions of members identified in mammalian cells (1). In humans, more than 30,000 piRNAs have been found, some of which map to hundreds or thousands of retrotransposable element–encoding genomic loci

(2–4). piRNAs are best characterized by their role in guiding PIWI proteins and associated chromatin-silencing machinery to transposon-encoding DNA sequences in the genome (5–7). This mechanism results in DNA methylation of piRNA targets in mammals, thereby repressing the activity of potentially destabilizing transposable elements in a heritable manner (5). We and others have suggested that a subset of piRNAs may also be capable of regulating protein-coding genes via DNA methylation, which may bear on cancer development if the regulatory targets are cancer-relevant (8–10).

Recent evidence suggests that the PIWI-piRNA system may also be active in certain somatic tissues and that its dysregulation or reactivation may be a factor in carcinogenesis (11, 12). PIWI family proteins have been shown to be aberrantly expressed and associated with poor prognosis in ovarian, colorectal, gastric, hepatocellular, esophageal, and pancreatic cancers (13–18), and piRNA expression has been observed in bladder, colon, lung, cervical, breast, hepatocellular, and gastric cancers (19–24). Our recent study also identified a genetic variant in a mature piRNA sequence that is associated with breast cancer risk (25). In the case of glioma, it has been shown that PIWI family gene *PIWIL1* displays oncogenic features in *in vitro* and *in vivo* glioma models (26) and that expression of the gene is associated with poor prognosis (27).

However, no study has explored the role that piRNAs may play in glioma development, despite the observation that some

¹Department of Environmental Health Sciences, Yale University School of Public Health, New Haven, Connecticut. ²Department of Chronic Disease Epidemiology, Yale University School of Public Health, New Haven, Connecticut. ³Department of Biostatistics, Yale University School of Public Health, New Haven, Connecticut. ⁴Department of Genetics, Yale Center for Genome Analysis, Yale University School of Medicine, New Haven, Connecticut. ⁵Yale Stem Cell Center and Department of Cell Biology, Yale University School of Medicine, New Haven, Connecticut.

Note: Supplementary data for this article are available at Cancer Epidemiology, Biomarkers & Prevention Online (<http://cebp.aacrjournals.org/>).

Current address for A. Fu: Department of Epidemiology, UCLA Fielding School of Public Health, Los Angeles, CA 90095.

Corresponding Author: Yong Zhu, Yale School of Public Health, 60 College Street, New Haven, CT 06510. Phone: 203-785-4844; Fax: 203-737-6023; E-mail: yong.zhu@yale.edu

doi: 10.1158/1055-9965.EPI-16-0047

©2016 American Association for Cancer Research.

piRNAs are expressed in normal mammalian brain specimens (28). The objective of this study was therefore to examine whether inherited variants in piRNA-encoding loci are associated with glioma risk using data from 1,840 glioma cases and 2,401 controls from the GliomaScan Cohort (29) and to examine the underlying basis for one of the observed associations using *in vitro* functional studies.

Materials and Methods

Study subjects and data

Individual-level genotype data and phenotypic subject characteristics for participants of the GliomaScan Cohort-based Genome-wide Association Study (29) were downloaded from the Database of Genotypes and Phenotypes (dbGaP, Study Accession phs000652.v1.p1) after receiving data access authorization. Subjects were restricted to those genotyped on the Illumina Human660W-Quad BeadChip to avoid potential bias introduced by the case-control imbalance of subjects genotyped on other platforms. After removal of related or duplicate subjects ($n = 25$ cases, $n = 150$ controls), there were 1,840 cases (ICDO-3 codes 9380-9480) and 2,401 controls included for final analysis.

Identification of piRNA variants

Genomic coordinates for all experimentally observed human piRNAs were obtained from the piRNABank database (30). SNPs included in the 1,000 Genomes Project Phase 3 (31) reference variant set ($n = 77,818,332$ biallelic SNPs) were identified within these coordinates. SNPs in piRNAs that map to more than 1,000 genomic loci were excluded, as these piRNAs may be less likely to be involved in protein-coding gene regulation (8).

piRNA variant genotype imputation

Genotype and phenotype data were downloaded to a secure server at Yale University and decrypted and extracted according to dbGaP guidelines. 1,000 Genomes Phase III haplotypes were downloaded for use as the reference panel for imputation using IMPUTE v2.3.1 software (32). Input data were restricted to SNPs with call rate $\geq 90\%$ and Hardy-Weinberg equilibrium HWE $P > 0.0001$ using the PLINK toolset (33). Fine mapping was conducted via imputation of all SNPs with minor allelic frequency (MAF) $> 1\%$ in 5-Mb chunks, and regional annotations were derived from the UCSC Genome Browser (34).

Statistical analysis for association study

ORs and 95% confidence intervals (CI) for variant-glioma associations were estimated with SNPTEST v2.5 software (35), applying an additive allelic logistic regression model adjusting for sex, age, study design, and the first two principal components. Principal components were generated by the smartPCA algorithm in the EIGENSOFT v6.0 population genetics package to adjust for residual population substructure (36). Associations surpassing a Bonferroni-corrected significance threshold were deemed statistically significant and associations yielding false discovery rate-adjusted $P < 0.10$ were considered to be modest associations of interest (37).

Experimental cell lines and reagents

Glioma cell lines U87 and A172 were purchased from ATCC and immortalized normal human astrocytes (NHA) were purchased from the University of California, San Francisco Tissue Core. All cell lines are tested for contaminants and authenticated prior to shipment using several characterization approaches including morphology assessment, karyotyping, cytochrome *c* oxidase variant analysis, and short tandem repeat DNA fingerprinting. Cells were not reauthenticated as they were passaged in our laboratory for fewer than 6 months after resuscitation. Cells were maintained in Eagle's modified essential medium (U87) or MEM (A172, NHA) and supplemented with 10% FBS. Single-stranded piRNA mimics were purchased from IDT (Supplementary Table S1), and single-stranded nontargeting RNA sequences of similar size were purchased from QIAGEN to act as negative controls in *in vitro* experiments. Cells were reverse-transfected using LipofectAMINE RNAiMAX transfection reagent (Invitrogen) according to the manufacturer's instructions.

Measurement of piRNA expression

Total RNA was isolated from U87, A172, and NHA cell lysates using the miRNeasy Mini Kit (QIAGEN), and cDNA was generated using the NCode miRNA First Strand cDNA Synthesis Kit (Invitrogen). qPCR was performed on an ABI-7500 System (Applied Biosystems) using a SYBR FAST qPCR Kit (Kapa Biosystems). Amplification reactions were conducted in triplicate with custom short piRNA forward primers and a universal reverse primer targeting appended poly(A) tails (Supplementary Table S1). Expression levels were normalized to small nuclear RNA U6 expression. Predicted secondary structures of piRNAs were generated by the Mfold v3.6 RNA folding algorithm using default parameters (38).

Genome-wide expression profiling

U87 cells were reverse transfected with either wild-type piR-598 or a nontarget control (NC) RNA. Cells were harvested 24 hours after transfection, and total RNA was isolated and approximately 1 μg was submitted to the Yale Center for Genome Analysis for genome-wide expression profiling on the Illumina HumanHT-12 v4 Expression BeadChip platform in biologic duplicate. Genes showing expression level differences between NC- and piR-598-WT treatments beyond a significance threshold of false discovery rate (FDR)-adjusted $P = 0.05$ were considered to be differentially expressed. Five genes were selected for expression validation by qPCR with input normalization to *GAPDH*. Network and pathway analyses were conducted using Ingenuity Pathway Analysis (IPA) software; P values for affected functional pathways were calculated using a Fisher exact test for enrichment of affected genes with a particular functional annotation. Array data have been deposited in the NCBI Gene Expression Omnibus repository (accession number GSE78935).

Cell viability assay

Cell viability was evaluated in piRNA-598- and negative control RNA-treated cell populations using the CellTiter 96 AQueous One Solution Cell Proliferation Assay (MTS) Kit (Promega). Briefly, cell viability was quantified at 48 and 96 hours after transfection. Color development was evaluated 1 hour after addition of MTS using a microplate spectrophotometer at an absorbance of

490 nm. Viability differences were analyzed using a Student's *t* test using six replicates per condition.

Soft agar colony formation assay

U87 cells were reverse-transfected with piRNA-598 or negative control oligos. Twenty-four hours after transfection, cells were trypsinized and resuspended in warmed EMEM with 0.36% agar. The mixture was plated in 60-mm cell culture dishes above a presolidified base layer of 0.75% agar. Dishes were incubated at 37°C with the addition of 500 μ L complete media every 5 days. After 3 weeks, colonies were stained with 0.04% crystal violet/2% ethanol in PBS and photographed. Colonies were counted using ImageJ v1.48 software and compared between conditions using a Student's *t* test. Experiments were performed in triplicate.

Results

Five piRNAs harbor glioma-associated germline variants

To determine whether inherited variants in piRNA-encoding sequences are associated with the risk of adult glioma development, a genetic association analysis was conducted in 1,840 subjects with newly diagnosed glioma and 2,401 cancer-free

controls included in the GliomaScan consortium. Approximately 67% of cases were diagnosed with high-grade glioma (grades III or IV), the majority of whom (82%) were of the glioblastoma multiforme subtype, and 55.2% of subjects were male (Supplementary Table S2).

A flowchart illustrating the selection of piRNA-sequence SNPs included in this analysis is presented in Supplementary Fig. S1. Of 2,514 SNPs of interest in piRNA-encoding sequences, 31 (1.2%) were directly genotyped on the Illumina Human-Hap660W platform, and genotypes at 1,397 (55.6%) were imputed; 1,086 SNPs (43.2%) were excluded because they were unable to be imputed with sufficiently high quality due to low array coverage in piRNA-encoding intergenic regions. In total, 1,428 SNPs were analyzed for association with glioma risk adjusting for sex, age, study design, and the first two principal components. No evidence of systematic bias from underlying population substructure or other factors was detected in the input genotype data using this model (genomic inflation factor, $\lambda = 1.009$; Supplementary Fig. S2).

A Manhattan plot illustrates all 1,428 piRNA SNP-glioma association test results (Fig. 1A). Our analysis revealed a Bonferroni-corrected ($P < 0.05/1,428 \text{ SNPs} = 3.50 \times 10^{-5}$) statistically

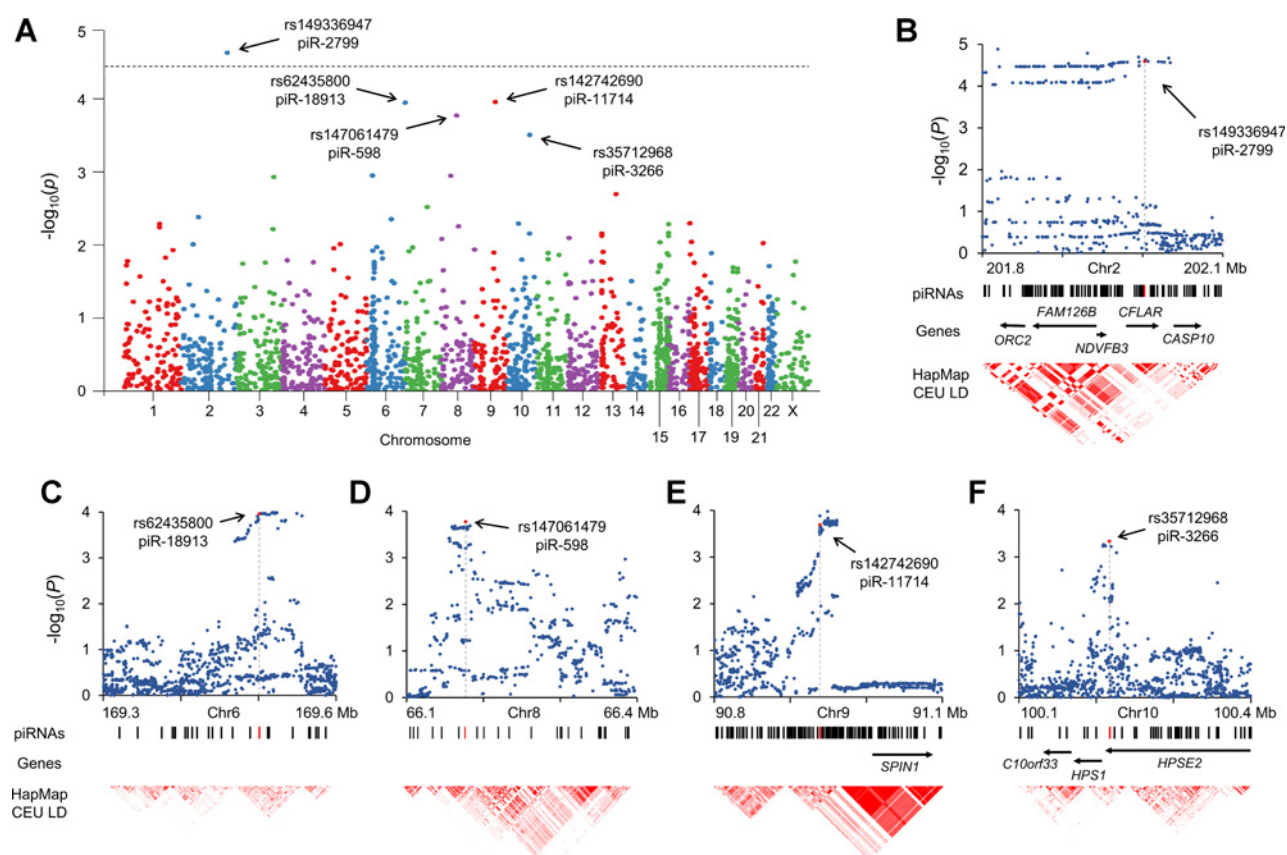


Figure 1.

Association analyses of piRNA variants and glioma. A, Manhattan plot of piRNA SNP-glioma association results. Five SNPs demonstrating statistically significant or suggestive associations with glioma risk are noted; dotted line represents the Bonferroni-adjusted significance threshold, $P = 3.50 \times 10^{-5}$. piRNA SNPs are plotted according to physical genomic order on the x-axis. B-F, regional imputation of all 1,000 Genomes SNPs with MAF > 1% in piR-2799, piR-18913, piR-598, piR-11714, and piR-3266 regions. Association results are presented in context of piRNAs from piRNABank, known protein-coding genes, and linkage disequilibrium (LD) patterns from the HapMap CEU population. Index SNPs and piRNAs are colored in red.

Table 1. Top piRNA SNPs associated with glioma risk by FDR-adjusted *P* value

rsID	piRNA	Chromosome band	Host gene	MAF(%) ^a	OR (95% CI) ^b	Nominal <i>P</i> value ^c	FDR-adjusted <i>P</i> value
rs149336947	piR-2799	2q33.1	<i>CFLAR</i>	0.8/1.6	2.54 (1.65–3.91)	2.34×10^{-5}	0.033
rs62435800	piR-18913	6q27	—	19.6/14.7	0.79 (0.70–0.89)	1.13×10^{-4}	0.054
rs147061479	piR-598	8q13.1	—	1.7/3.1	1.80 (1.33–2.46)	1.69×10^{-4}	0.060
rs142742690	piR-11714	9q22.1	—	7.2/5.1	0.69 (0.57–0.83)	1.10×10^{-4}	0.079
rs35712968	piR-3266	10q24.2	<i>HPSE2</i>	4.3/3.1	0.64 (0.51–0.82)	3.11×10^{-4}	0.089

^aControls/cases.^bAssociations were calculated by logistic regression under an additive allelic model adjusting for sex, age, study design, and the first two principal components.^cBonferroni-corrected $P = 3.50 \times 10^{-5}$.

significant association between glioma risk and rare variant rs149336947 ($P = 2.34 \times 10^{-5}$; FDR-adjusted $P = 0.033$), located near the 3' end of piR-2799 on chromosome 2q33.1. piR-2799 is a 30-nucleotide piRNA that maps to the fourth intron of apoptosis inhibitor *CFLAR*, which is widely expressed in the human body including in the brain (39).

Four additional modest associations of interest were observed at rs62435800 in piR-18913 on chromosome 6q27 ($P = 1.13 \times 10^{-4}$; FDR-adjusted $P = 0.054$), rs147061479 in piR-598 on chromosome 8q13.1 ($P = 1.69 \times 10^{-4}$; FDR-adjusted $P = 0.060$), rs142742690 in piR-11714 on chromosome 9q22.1 ($P = 1.10 \times 10^{-4}$; FDR-adjusted $P = 0.079$), and rs35712968 in piR-3266 on chromosome 10q24.2 ($P = 3.11 \times 10^{-4}$; FDR-adjusted $P = 0.089$; Table 1).

To examine these associations at higher resolution, genotypes were imputed for all SNPs in 300-kb regions surrounding the five associated SNPs. For piR-2799, this analysis revealed nearly 100 SNPs with associations of comparable magnitude to that of rs149336947 spanning a 250-kb region of linkage disequilibrium (Fig. 1B). This region contains four genes and is upstream of one gene. In contrast, clusters of SNPs showing enhanced association signals were observed in more narrow regions of linkage disequilibrium surrounding rs62435800 in piR-18913, rs147061479 in piR-598, rs142742690 in piR-11714, and rs35712968 in piR-3266 (Fig. 1C–F). Both piR-18913 and piR-598 map to genetic regions that encode a small number of piRNAs and are devoid of protein-coding genes. piR-11714 is located on a piRNA-dense haplotype that does not encode protein-coding genes and is approximately 50 kb upstream of *SPIN1*, and piR-3266 maps to the 3' untranslated region (UTR) of *HPSE2*.

Expression of four piRNAs identified in glial cell lines

piRNA expression measurement was conducted using a qPCR-based method. Results showed expression of piR-18913, piR-598, piR-11714, and piR-3266 in all cell lines tested (U87, A172, and NHA; Supplementary Fig. S3). Expression of piR-2799 was not detected in any of the cell lines.

piR-598 impacts multiple glioma-relevant functional pathways

Among the four candidate piRNAs (piR-18913, piR-598, piR-11714, and piR-3266) that were found to be expressed in the cell lines examined, piR-598 harbored the variant conferring the greatest magnitude of glioma risk or protection and therefore was the subject of additional *in vitro* functional analyses. The predicted secondary structure of piR-598 is illustrated in Fig. 2A. In the most thermodynamically stable structure, the piRNA forms a small hairpin loop from the 5th

to 19th bases; variant rs147061479, located at the 29th of 31 bases, is not involved in the predicted loop structure. We performed transcriptome-wide expression profiling 24 hours after transient upregulation of the piRNA in U87 cells to examine the impact of the expression of this piRNA in the context of glioma. Relative to nontargeting control-treated cells, a total of 518 transcripts were observed to be differentially expressed at FDR-adjusted $P < 0.05$ (Supplementary Table S3), the majority of which (71.2%) were observed to be underexpressed in piR-598-treated cells. Expression differences for five transcripts selected for validation of expression array data by qPCR were generally consistent with array results (Supplementary Fig. S4).

Subsequent pathway analysis showed that piR-598-affected genes were significantly enriched for those involved in cell death and survival ($P = 3.43 \times 10^{-3}$), cell-cycle progression ($P = 2.63 \times 10^{-3}$), and cellular assembly and organization ($P = 2.39 \times 10^{-3}$; Fig. 2B). Network visualization analysis revealed a core of functionally interrelated molecules including *BAX*, a key regulator of p53-mediated apoptosis, and oncogenic transcription factor *JUN* (Fig. 2C).

SNP rs147061479 impacts piR-598 function in cell viability and colony formation

Wild-type and variant piR-598 mimics were independently overexpressed in glioma (U87 and A172) and NHA cell lines, and cell viability was measured. Relative to a nontargeting control RNA, transfection of wild-type piR-598 sharply reduced proliferation of both U87 and A172 cells, notably with nearly 40% inhibition measured 96 hours after transfection in U87. However, transfection of the mutant rather than wild-type piR-598, containing the variant allele, significantly attenuated the antiproliferative impact. The same pattern was observed in normal glial cell line NHA (Fig. 3A).

The functional impact of the piRNA variant was also examined on U87 colony formation in soft agar, which is a model of anchorage-independent growth potential. Treatment with wild-type piR-598 reduced the number of colonies formed to approximately half those formed following negative control treatment. However, treatment with the variant rather than wild-type piRNA was sufficient to not only eliminate the anti-proliferative effect of the piRNA but also confer a more than 4-fold increased colony-forming potential relative to wild-type piR-598 treatment (Fig. 3B).

Discussion

This post-GWAS study suggests that inherited variants at five piRNA loci (FDR-adjusted $P < 0.10$) are associated with glioma

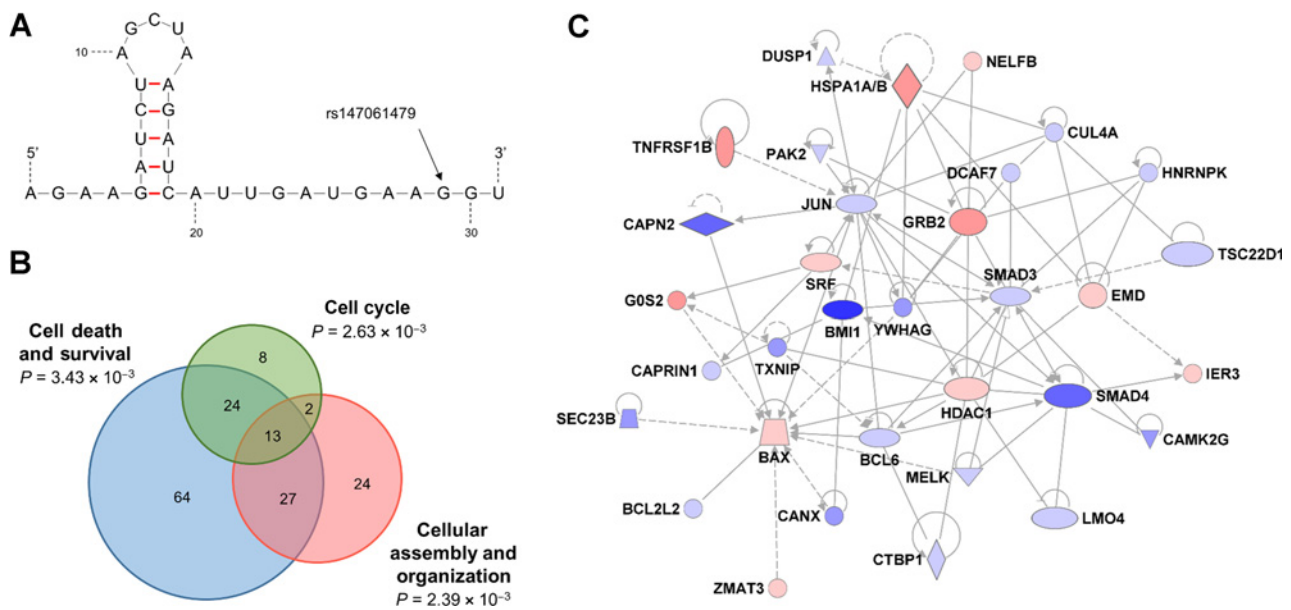


Figure 2.

piR-598 structure and transcriptional impact. A, predicted secondary structure of piR-598 and location of rs147061479. Illustration was adapted from prediction by the Mfold v.3.6 RNA folding algorithm. Paired bases are denoted by red connecting lines. B, transcripts affected by overexpression of piR-598 mimics in U87 were enriched for those with roles in the indicated molecular functions according to IPA. *P* values were generated using Fisher's exact test for enrichment of affected genes according to functional annotation. C, network visualization illustrating functional interrelatedness of differentially expressed transcripts related to cell death and cell-cycle progression following piR-598 treatment of U87 cells. Red and blue shading denote piR-598-induced transcript over- and underexpression relative to negative control, respectively, with color intensity corresponding to degree of change; solid lines and dotted lines indicate direct and indirect relationships, respectively.

risk in the GliomaScan Cohort, the largest publicly available glioma GWAS dataset. None of these associations has been reported in previous publications. Genomic loci at 8q24 and 9p21 have been linked to glioma in previous GWAS (40, 41); however, observed associations on these chromosomes at rs147061479 (piRNA-598 at 8q13) and rs142742690 (piRNA-11714 at 9q22) are unrelated to previous signals, suggesting that novel genetic risk loci harboring piRNA variants have been identified from our post-GWAS approach.

A Bonferroni-adjusted significant association was detected between glioma risk and rs149336947 in piR-2799. Regional imputation showed that this association extended over a large region of linkage disequilibrium that harbors four genes including apoptosis regulator *CFLAR*, as well as the promoter region for initiator caspases *CASP10* and *CASP8* that has been linked to susceptibility to several cancers (42). Thus, the association at rs149336947 may reflect a functional polymorphism that is unrelated to piR-2799, possibly representing a separate low-frequency biomarker of glioma risk that is itself worthy of further follow-up. The observation that piR-2799 expression was undetectable in U87, A172, or NHA cell lines further supports this notion.

In contrast, regional imputation of the other four regions harboring piRNAs piR-18913, piR-598, piR-11714, and piR-3266 revealed narrow clusters of SNPs with amplified association signals relative to surrounding areas. There are no protein-coding genes in the regions that encode piR-598 and piR-18913. Moreover, expression of all four of these piRNAs was detectable in both normal glial and glioma cell lines. These findings suggest potential biologic roles of these piRNAs and

their variants in gliomagenesis that warrants further examination.

The functional significance of one of the identified piRNAs, piR-598, was explored in follow-up transcriptional profiling and network analyses, which indicated involvement of this piRNA in cell death and survival pathways. Of particular interest was the upregulated expression of the *BAX* transcript, which encodes a protein that promotes cell death by inhibiting apoptosis repressor Bcl-2 (43). Expression of the closely related *GOS2* gene, encoding another Bcl-2-interacting and apoptosis-promoting protein (44), was upregulated. We performed expression profiling after a relatively short treatment period (24 hours) to detect early piRNA-induced transcriptional changes before cell viability was compromised; gene expression differences in this experiment did not tend to be large in magnitude as a result.

Subsequent *in vitro* assays confirmed the role of piR-598 in cellular growth identified from the expression profiling analysis and further demonstrated the functional impact of the genetic variant. Delivery of the wild-type piRNA-598 mimic significantly diminished cell viability relative to control treatment. However, upregulation of the variant rather than wild-type piR-598 sharply attenuated the antiproliferative response observed with the wild-type piRNA. Additional evidence comes from the observation that wild-type piR-598 treatment limited long-term colony formation of U87 cells seeded in soft agar, yet treatment instead with the variant piRNA was sufficient to eliminate the antiproliferative effect of piR-598 and in fact promoted colony formation. The discrepancy in the effect of the variant piRNA with respect

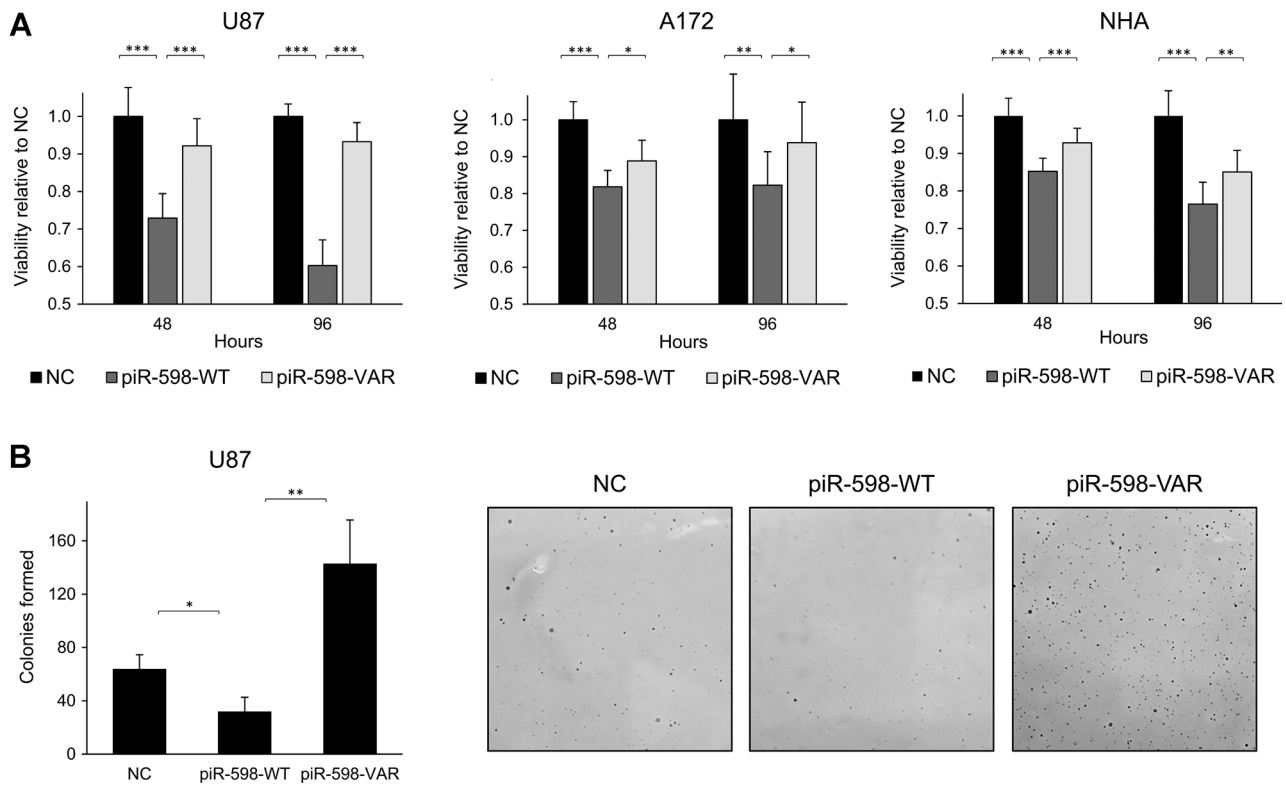


Figure 3. Glial cell viability and soft agar colony formation following wild-type (WT) or variant (V) piR-598 treatment. A, approximately 2.5×10^3 U87, A172, or NHA cells were transfected with 25 nmol/L piR-598-WT or piR-598-V mimics or a control RNA oligo in 96-well plates with 6 replicates per condition. Cell viability was quantified using MTS at 48 and 96 hours after transfection. B, approximately 1×10^4 cells were transfected with indicated oligos and seeded in triplicate 24 hours later in soft agar in a single-cell suspension. Colonies were counted using ImageJ 3 weeks after seeding. Representative images of colonies formed in each treatment condition are shown. NC, negative control. *, $P < 0.05$; **, $P < 0.01$; ***, $P < 0.001$; error bars denote SD of replicate experiments.

to negative control treatment in the two assays was likely attributable to the difference in time period of cell growth after piRNA treatment (4 vs. 21 days), as an increased growth rate attributable to the variant piRNA was more readily revealed via the greater number of population doublings occurring in the longer term colony formation assay. These results provide consistent functional support for the increased glioma risk associated with rs147061479.

While these post-GWAS and functional analyses suggest a role of PIWI-interacting RNAs in gliomagenesis, the current study has some limitations. Although the association at rs147061479 in piR-598 is supported by follow-up functional analyses, we recognize that replication of the piR-598 association in an independent population would provide additional support for its role in gliomagenesis. Furthermore, because of the unavailability of individual-level glioma subtype data, we were unable to explore subtype-specific associations despite the widely accepted heterogeneity of the disease. However, *in vitro* analyses of piR-598 were performed in cell line models of grade IV glioma, supporting a role for the rs147061479 variant in this subtype. In addition, genotypes of glioma-associated piRNA SNPs were imputed rather than directly genotyped; however, we utilized a strict threshold for imputation quality and accounted for genotype uncertainty in our model, thus result-

ing in appropriately conservative association estimates. Finally, additional mechanistic work will be required to uncover the precise molecular basis for the observed genetic associations and phenotypic impact of piR-598. We and others have demonstrated that piRNAs may be capable of inducing DNA methylation of protein-coding genes (8, 10), and PIWI family protein PIWIL4 has been shown to localize to the nucleus and may be involved in *de novo* DNA methylation of transposable elements (45) as well as targeted protein-coding genes. It has also been suggested that certain PIWI-piRNA complexes may have siRNA-like roles as posttranscriptional regulators in mRNA degradation and translational regulation (1, 46). Establishing the direct targets of piRNAs in a cancer context is an important area for future investigation.

In summary, this multidisciplinary study demonstrates a novel role of piRNAs, a group of small noncoding RNAs, in gliomagenesis using evidence from both post-GWAS and *in vitro* functional analyses. These findings add to a growing body of research linking the PIWI-piRNA pathway and human cancer and strongly support expanded exploration of this abundant yet relatively understudied class of noncoding RNA in relation to cancer development. Pursuing this research may yield novel biomarkers for cancer risk, insights into the tumor developmental process, and strategies for cancer treatment.

Disclosure of Potential Conflicts of Interest

No potential conflicts of interest were disclosed.

Authors' Contributions

Conception and design: D.I. Jacobs, A. Fu, R. Dubrow, H. Lin, Y. Zhu
Development of methodology: D.I. Jacobs, Q. Qin, Y. Zhu
Acquisition of data (provided animals, acquired and managed patients, provided facilities, etc.): D.I. Jacobs, Q. Qin, G. Wang, Y. Zhu
Analysis and interpretation of data (e.g., statistical analysis, biostatistics, computational analysis): D.I. Jacobs, A.T. DeWan, H. Lin, Y. Zhu
Writing, review, and/or revision of the manuscript: D.I. Jacobs, Q. Qin, A. Fu, R. Dubrow, E.B. Claus, A.T. DeWan, G. Wang, H. Lin, Y. Zhu
Administrative, technical, or material support (i.e., reporting or organizing data, constructing databases): Y. Zhu
Study supervision: E.B. Claus, H. Lin, Y. Zhu

Grant Support

This work was supported by the NCI grant CA122676 and funds from Yale University. D.I. Jacobs was supported by the Yale-NCI predoctoral training grant T32 CA105666. A. Fu was partially supported by UCLA-NCI training grant T32 CA09142. E.B. Claus was partially supported by CA119215.

The costs of publication of this article were defrayed in part by the payment of page charges. This article must therefore be hereby marked *advertisement* in accordance with 18 U.S.C. Section 1734 solely to indicate this fact.

Received January 26, 2016; revised March 31, 2016; accepted April 4, 2016; published OnlineFirst May 13, 2016.

References

- Watanabe T, Cheng EC, Zhong M, Lin H. Retrotransposons and pseudogenes regulate mRNAs and lncRNAs via the piRNA pathway in the germline. *Genome Res* 2015;25:368–80.
- Ku H-Y, Lin H. PIWI proteins and their interactors in piRNA biogenesis, germline development and gene expression. *Nat Sci Rev* 2014;1:205–18.
- Aravin A, Gaidatzis D, Pfeffer S, Lagos-Quintana M, Landgraf P, Iovino N, et al. A novel class of small RNAs bind to MILI protein in mouse testes. *Nature* 2006;442:203–7.
- Girard A, Sachidanandam R, Hannon GJ, Carmell MA. A germline-specific class of small RNAs binds mammalian Piwi proteins. *Nature* 2006;442:199–202.
- Aravin AA, Sachidanandam R, Girard A, Fejes-Toth K, Hannon GJ. Developmentally regulated piRNA clusters implicate MILI in transposon control. *Science* 2007;316:744–7.
- Huang XA, Yin H, Sweeney S, Raha D, Snyder M, Lin H. A major epigenetic programming mechanism guided by piRNAs. *Dev Cell* 2013;24:502–16.
- Yin H, Lin H. An epigenetic activation role of Piwi and a Piwi-associated piRNA in *Drosophila melanogaster*. *Nature* 2007;450:304–8.
- Fu A, Jacobs DI, Zhu Y. Epigenome-wide analysis of piRNAs in gene-specific DNA methylation. *RNA Biol* 2014;11:1301–12.
- Rajasekharan P, Antonov I, Sheridan R, Frey S, Sander C, Tuschl T, et al. A role for neuronal piRNAs in the epigenetic control of memory-related synaptic plasticity. *Cell* 2012;149:693–707.
- Watanabe T, Tomizawa S-i, Mitsuya K, Totoki Y, Yamamoto Y, Kuramochi-Miyagawa S, et al. Role for piRNAs and noncoding RNA in de novo DNA methylation of the imprinted mouse *Rasgrf1* locus. *Science* 2011;332:848–52.
- Siddiqi S, Matushansky I. Piwis and piwi-interacting RNAs in the epigenetics of cancer. *J Cell Biochem* 2012;113:373–80.
- Moyano M, Stefani G. piRNA involvement in genome stability and human cancer. *J Hematol Oncol* 2015;8:38.
- Lu L, Katsaros D, Risch HA, Canuto EM, Biglia N, Yu H. MicroRNA let7a modifies the effect of self-renewal gene HIWI on patient survival of epithelial ovarian cancer. *Mol Carcinog* 2016;55:357–65.
- Oh S-J, Kim S-M, Kim Y-O, Chang H-K. Clinicopathologic implications of PIWIL2 expression in colorectal cancer. *Korean J Pathol* 2012;46:318–23.
- Wang Y, Liu Y, Shen X, Zhang X, Chen X, Yang C, et al. The PIWI protein acts as a predictive marker for human gastric cancer. *Int J Clin Exp Pathol* 2012;5:315.
- Zhao YM, Zhou JM, Wang LR, He HW, Wang XL, Tao ZH, et al. HIWI is associated with prognosis in patients with hepatocellular carcinoma after curative resection. *Cancer* 2012;118:2708–17.
- He W, Wang Z, Wang Q, Fan Q, Shou C, Wang J, et al. Expression of HIWI in human esophageal squamous cell carcinoma is significantly associated with poorer prognosis. *BMC Cancer* 2009;9:426.
- Grochola L, Greither T, Taubert H, Möller P, Knippschild U, Udelnow A, et al. The stem cell-associated Hiwi gene in human adenocarcinoma of the pancreas: expression and risk of tumour-related death. *Br J Cancer* 2008;99:1083–8.
- Chu H, Hui G, Yuan L, Shi D, Wang Y, Du M, et al. Identification of novel piRNAs in bladder cancer. *Cancer Lett* 2015;356:561–7.
- Hashim A, Rizzo F, Marchese G, Ravo M, Tarallo R, Nassa G, et al. RNA sequencing identifies specific PIWI-interacting small non-coding RNA expression patterns in breast cancer. *Oncotarget* 2014;5:9901.
- Law PT, Qin H, Ching AK, Lai KP, Co NN, He M, et al. Deep sequencing of small RNA transcriptome reveals novel non-coding RNAs in hepatocellular carcinoma. *J Hepatol* 2013;58:1165–73.
- Huang G, Hu H, Xue X, Shen S, Gao E, Guo G, et al. Altered expression of piRNAs and their relation with clinicopathologic features of breast cancer. *Clin Transl Oncol* 2013;15:563–8.
- Cheng J, Deng H, Xiao B, Zhou H, Zhou F, Shen Z, et al. piR-823, a novel non-coding small RNA, demonstrates *in vitro* and *in vivo* tumor suppressive activity in human gastric cancer cells. *Cancer Lett* 2012;315:12–7.
- Cheng J, Guo JM, Xiao BX, Miao Y, Jiang Z, Zhou H, et al. piRNA, the new non-coding RNA, is aberrantly expressed in human cancer cells. *Clin Chim Acta* 2011;412:1621–5.
- Fu A, Jacobs DI, Hoffman AE, Zheng T, Zhu Y. PIWI-interacting RNA 021285 is involved in breast tumorigenesis possibly by remodeling the cancer epigenome. *Carcinogenesis* 2015;36:1094–102.
- Wang X, Tong X, Gao H, Yan X, Xu X, Sun S, et al. Silencing HIWI suppresses the growth, invasion and migration of glioma cells. *Int J Oncol* 2014;45:2385–92.
- Sun G, Wang Y, Sun L, Luo H, Liu N, Fu Z, et al. Clinical significance of Hiwi gene expression in gliomas. *Brain Res* 2011;1373:183–8.
- Lee EJ, Banerjee S, Zhou H, Jammalamadaka A, Arcila M, Manjunath BS, et al. Identification of piRNAs in the central nervous system. *RNA* 2011;17:1090–9.
- Rajaraman P, Melin BS, Wang Z, McKean-Cowdin R, Michaud DS, Wang SS, et al. Genome-wide association study of glioma and meta-analysis. *Hum Genet* 2012;131:1877–88.
- Sai Lakshmi S, Agrawal S. piRNABank: a web resource on classified and clustered Piwi-interacting RNAs. *Nucleic Acids Res* 2008;36:D173–D7.
- 1000 Genomes Project Consortium, Abecasis GR, Auton A, Brooks LD, DePristo MA, Durbin RM, et al. An integrated map of genetic variation from 1,092 human genomes. *Nature* 2012;491:56–65.
- Howie BN, Donnelly P, Marchini J. A flexible and accurate genotype imputation method for the next generation of genome-wide association studies. *PLoS Genet* 2009;5:e1000529.
- Purcell S, Neale B, Todd-Brown K, Thomas L, Ferreira MAR, Bender D, et al. PLINK: a tool set for whole-genome association and population-based linkage analyses. *Am J Hum Genet* 2007;81:559–75.
- Rosenbloom KR, Armstrong J, Barber GP, Casper J, Clawson H, Diekhans M, et al. The UCSC Genome Browser database: 2015 update. *Nucleic Acids Res* 2015;43:D670–D81.
- Marchini J, Howie B. Genotype imputation for genome-wide association studies. *Nat Rev Genet* 2010;11:499–511.
- Patterson N, Price AL, Reich D. Population structure and eigenanalysis. *PLoS Genet* 2006;2:e190.
- Benjamini Y, Hochberg Y. Controlling the false discovery rate: a practical and powerful approach to multiple testing. *J Roy Stat Soc Series B (Methodological)* 1995;57:289–300.
- Zuker M. Mfold web server for nucleic acid folding and hybridization prediction. *Nucleic Acids Res* 2003;31:3406–15.

39. Lonsdale J, Thomas J, Salvatore M, Phillips R, Lo E, Shad S, et al. The Genotype-Tissue Expression (GTEx) project. *Nat Genet* 2013;45:580–5.
40. Wrensch M, Jenkins RB, Chang JS, Yeh R-F, Xiao Y, Decker PA, et al. Variants in the CDKN2B and RTEL1 regions are associated with high-grade glioma susceptibility. *Nat Genet* 2009;41:905–8.
41. Shete S, Hosking FJ, Robertson LB, Dobbins SE, Sanson M, Malmer B, et al. Genome-wide association study identifies five susceptibility loci for glioma. *Nat Genet* 2009;41:899–904.
42. Sun T, Gao Y, Tan W, Ma S, Shi Y, Yao J, et al. A six-nucleotide insertion-deletion polymorphism in the CASP8 promoter is associated with susceptibility to multiple cancers. *Nat Genet* 2007;39:605–13.
43. Oltval ZN, Milliman CL, Korsmeyer SJ. Bcl-2 heterodimerizes *in vivo* with a conserved homolog, Bax, that accelerates programmed cell death. *Cell* 1993;74:609–19.
44. Welch C, Santra MK, El-Assaad W, Zhu X, Huber WE, Keys RA, et al. Identification of a protein, GOS2, that lacks Bcl-2 homology domains and interacts with and antagonizes Bcl-2. *Cancer Res* 2009;69:6782–9.
45. Aravin AA, Van Der Heijden GW, Castañeda J, Vagin VV, Hannon GJ, Bortvin A. Cytoplasmic compartmentalization of the fetal piRNA pathway in mice. *PLoS Genet* 2009;5:e1000764–e.
46. Grivna ST, Pyhtila B, Lin H. MIWI associates with translational machinery and PIWI-interacting RNAs (piRNAs) in regulating spermatogenesis. *Proc Natl Acad Sci* 2006;103:13415–20.